

Article

Parameter Optimization of Wireless Power Transfer Based on Machine Learning

Heng Zhang ^{1,†} , Manwen Liao ^{2,†}, Liangxi He ¹ and Chi-Kwan Lee ^{1,*}

¹ The Department of Electrical and Electronic Engineering, The University of Hong Kong, Hong Kong 999077, China; zhhku@connect.hku.hk (H.Z.); u3005900@connect.hku.hk (L.H.)

² The Department of Computer Science, The University of Hong Kong, Hong Kong 999077, China; manwen@connect.hku.hk

* Correspondence: ckleee@eee.hku.hk

† These authors contributed equally to this work.

Abstract: Wireless power transfer (WPT) has become a crucial feature in numerous electronic devices, electric appliances, and electric vehicles. However, traditional design methods for WPT suffer from numerous drawbacks, such as time-consuming computations and high error counts due to inaccurate model parameters. As artificial intelligence (AI) continues to gain traction across industries, its ability to provide quick decisions and solutions makes it highly attractive for system optimizations. In this paper, a method for optimizing WPT parameters based on machine learning is proposed. The convolutional neural network is adapted for training and predicting the performance of a pair of coupled coils under a set of input parameters. The performance parameters include the spatial magnetic field distribution map, quality factor, inductance value, and mutual inductance value, which are critical in determining the efficiency and selecting optimal coil parameters such as the number of turns and wire diameter. Moreover, the spatial magnetic field distribution map is also helpful for identifying design compliance with the electromagnetic field safety standards. The training results reveal that the proposed method takes an average of 3.2 ms with a normalized image prediction error of 0.0034 to calculate the results to calculate one set of parameters, compared to an average of 23.74 s via COMSOL. This represents significant computational time savings while still maintaining acceptable computational accuracy.

Keywords: parameter optimization; machine learning; wireless power transfer



Citation: Zhang, H.; Liao, M.; He, L.; Lee, C.-K. Parameter Optimization of Wireless Power Transfer Based on Machine Learning. *Electronics* **2024**, *13*, 103. <https://doi.org/10.3390/electronics13010103>

Academic Editors: Yong Li, Yanling Li, Linlin Tan and Xing Zhao

Received: 8 December 2023

Revised: 20 December 2023

Accepted: 22 December 2023

Published: 26 December 2023



Copyright: © 2023 by the authors. Licensee MDPI, Basel, Switzerland. This article is an open access article distributed under the terms and conditions of the Creative Commons Attribution (CC BY) license (<https://creativecommons.org/licenses/by/4.0/>).

1. Introduction

Wireless power transfer (WPT) technology is gaining increasing attention from academia and industry [1]. At present, this technology is widely used in various wireless power supply applications, including IoT batteryless sensors or devices [2,3], portable consumer electronics such as wearable devices and mobile phones [4–6], and automation equipment such as electric vehicles and robots [7,8], as well as electrical equipment in implantable biomedicine, underwater, mining, and aerospace applications [9–12]. The terminals of the WPT systems cover electrical loads ranging from microwatts to megawatts. Traditional methods for optimizing inductors for WPT include full analytical models, semi-numerical models, and numerical models [13]. Sometimes, however, these three methods cannot meet all the requirements, so it is necessary to propose an optimal wireless power supply parameter selection method based on machine learning (ML).

In recent years, the three traditional methods for circuit parameter optimization [14] have shown some drawbacks. As for the first method, full analytical models [15,16], these models are based on analytical equations and feature closed-form analytical solutions. These models are too simple to fully express the circuit properties of a circuit, so the disadvantage is that they are not accurate for prototyping. Semi-numerical models [17, 18] are based on analytical equations but do not feature an explicit solution. Obtaining

the optimal design is accomplished by numerical optimization methods (e.g., gradient optimization and brute force). This numerical optimization is accurate and fairly fast. However, the mechanisms that lead to optimal designs are difficult to define. In addition, the results obtained are specific to a given specification and cannot be easily generalized. When it comes to numerical models [16,19,20], the WPT parameters are extracted from numerical field simulations (e.g., finite element method simulations). This method is relatively accurate, but modeling and model computation are time-consuming and offer only limited advantages over semi-numerical methods [21].

Fortunately, artificial intelligence (AI) has become increasingly popular [22,23] and has recently been applied to some fields of power electronics design, showing the future development trend of AI in power electronics, such as modeling B-H loops of power magnetics with sequence-to-sequence LSTM encoder–decoder architectures [24], deep reinforcement learning for DC-DC converter parameter optimization [25], and machine learning estimators for power electronics design and optimization [26]. These successful examples inspired us to employ the AI approach for the design of a WPT optimal parameter analysis method.

Therefore, applying machine learning methods to resolve the challenge of WPT parameter optimization presents great potential. This paper proposes the parameter optimization of WPT based on machine learning (POWPTML). The principal contributions of this paper are outlined below:

- (1) The computational efficiency in selecting WPT circuit parameters is significantly enhanced, concurrently achieving a small error margin.
- (2) The machine learning techniques are employed to rapidly generate a magnetic field distribution map under the specific coil and current conditions, which is a crucial factor for ensuring safety.

The organization of this paper is as follows: Section 2 introduces the parameter requirements of magnetic field distribution and efficiency optimization for WPT. The machine learning framework and training configurations are described in Section 3. The results of COMSOL and POWPTML and their comparison are shown in Section 4. The feasibility of the method proposed in this paper is verified through the experiments described in Section 5. The Discussion and Conclusions are presented in Sections 6 and 7, respectively. Codes for our implementation are available at [GitHub](#) (accessed on 20 December 2023).

2. Parameter Requirements and Optimization of WPT

In the design of WPT, electromagnetic environmental issues or efficiency issues need to be considered in a variety of cases.

2.1. Magnetic Field Distribution

The distribution of changing magnetic fields has bad effects on the human body and mechanical or electronic devices. Therefore, the International Commission on Non-Ionizing Radiation Protection (ICNIRP) was established in 1992 to study the biological effects of various types of non-ionizing radiation. In 1998 “Guidelines for limiting exposure to time-varying electric, magnetic, and electromagnetic fields (up to 300 GHz)” was issued [27]. As the most representative electromagnetic wave radiation standard in the world, it refers to a large number of literature studies on the biological effects of exposure to static and low-frequency electromagnetic fields. In 2010, the “Guidelines for limiting exposure to time-varying electric and magnetic fields (1 Hz to 100 kHz)” [28] was promulgated, which revised the safety guidelines for the electromagnetic protection of the human body exposed to low-frequency electric and magnetic fields.

In addition, WPT is one of the most promising technologies for electric vehicle (EV) charging applications [29]; thus, the Society of Automotive Engineers (SAE) published the SAE J2954 standard for the better development of WPT in EV [30]. SAE J2954 recommends limiting electromagnetic field emissions below the limits established in the ICNIRP-2010 guidelines, as given in Table 1. Therefore, the prediction of magnetic field distribution

is crucial to ensuring the safety of humans and devices when AI performs parameter optimization design.

Table 1. ICNIRP 2010 limits on the low-frequency electromagnetic field.

Field Type	General Public Reference Limit
Magnetic	27 μT RMS or 38 μT peak
Electric field	RMS 83 V/m

In the wireless transmission of electrical energy, the magnetic field generated by the transmitting coil plays a pivotal role in charging efficiency. As the distance between the transmitting and receiving coils increases, the magnetic field strength diminishes, resulting in reduced energy reception for a given set of coil parameters. Therefore, the analysis of magnetic field distribution serves as an indicator for assessing wireless charging performance at different locations. Additionally, the distribution diagram of alternating magnetic fields can be employed to delineate the safety boundaries of the magnetic field.

2.2. WPT Efficiency

The circuit topologies used in a two-coil magnetically coupled resonant WPT system can be divided into four types [31,32]: primary-side and secondary-side capacitor–inductor series resonance (SS type); primary-side capacitor–inductor series, secondary-side capacitor–inductor parallel resonance (SP type); primary-side capacitor–inductor parallel, secondary-side capacitor–inductor series resonance (PS type); and primary-side and secondary-side capacitor–inductor parallel resonance (PP type). Based on several studies, the most popular circuit topology is SS [33]. An SS-type topology circuit diagram is shown in Figure 1.

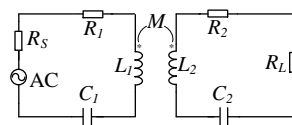


Figure 1. Capacitor–inductor series resonance. (‘*’ representing the dotted terminal of mutual inductance).

When the two coils L_1 and L_2 perform magnetic coupling resonant wireless power transmission, the transfer efficiency η can be expressed [34] as

$$\eta = \frac{R_L}{(R_L + R_2)} \frac{(\omega M)^2}{(\omega M)^2 + (R_S + R_1)(R_L + R_2)} \tag{1}$$

$$= \frac{R_L}{(R_L + R_2)} \frac{k^2 Q_1 Q_2}{(1 + k^2 Q_1 Q_2)},$$

where R_S is the internal resistance of the power supply; R_1 is the internal resistance of the transmitting coil; R_2 is the internal resistance of the receiving coil; R_L is the load resistance; M is the mutual inductance value between the transmitting and receiving coils; ω is the resonant angular frequency; Q_1 is the quality factor of L_1 ; and Q_2 is the quality factor of L_2 . The coupling coefficient k can be expressed as

$$k = \frac{M}{\sqrt{L_1 L_2}}. \tag{2}$$

In most cases, R_L is much larger than R_2 , so η can be abbreviated as

$$\eta \approx \frac{k^2 Q_1 Q_2}{1 + k^2 Q_1 Q_2} = \frac{1}{1 + \frac{1}{k^2 Q_1 Q_2}}. \tag{3}$$

It can be seen from Equation (3) that the highest efficiency can be obtained by finding the maximum value of $k^2 Q_1 Q_2$.

3. Machine Learning for WPT

We apply machine learning to learn the distribution of magnetic fields. A deep neural network [35] is well known for its strong function approximation ability. It is widely applied in fields like computer vision and natural language processing. In our framework, we transform the intensity of magnetic fields into gray images. The neural network takes as input the parameters of coils. Then, it predicts the image representation of magnetic field distribution and the coil parameters.

3.1. Machine Learning Framework

As shown in Figure 2, our proposed machine learning framework utilizes a U-Net-based [36] structure to learn the magnetic field distribution and a multi-layer perceptron (MLP) [37] branch to predict the optimal parameters.

U-Net was first proposed to solve semantic segmentation tasks [38] in computer vision. The original form of U-Net translates an image into its semantic segmentation map. The segmentation map consists of pixels indicating whether they belong to the same object category or not. It could be regarded as a spatial distribution of categories, which resembles our target spatial distribution of magnetic fields. One difference is that the magnetic field distribution is continuous. The U-Net contains two sub-modules, namely, an encoder and a decoder, both of which are built up with convolutional blocks. The encoder down-samples the input image into a low-dimensional feature vector, whereas the decoder up-samples the feature vector and constructs a high-dimensional segmentation map.

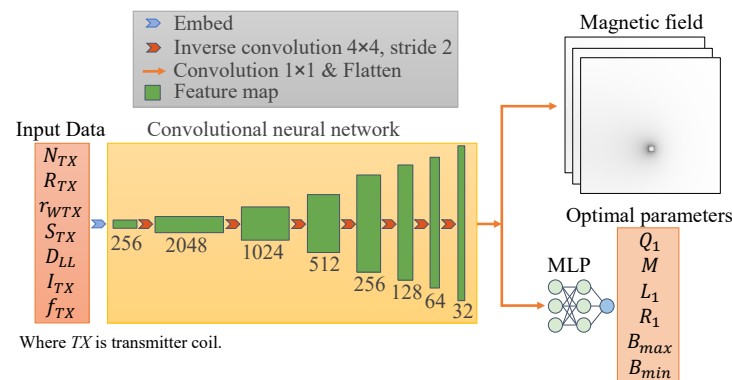


Figure 2. Diagram of our machine learning model structure.

In our framework, since the neural network maps numerical data into images, we only use the decoder part of U-Net. Here, we adapt its ability to decode rich semantic information in low-dimensional vectors to generate the spatial distribution of magnetic fields. Specifically, the input and output of our model are shown in Figure 2. The input is first linearly transformed (embedded) into a high-dimensional vector representation. Then, two separate branches are followed to predict magnetic field distribution and optimal parameters, respectively.

For field prediction, we up-sample the high-dimensional vector into an image-like feature vector. The up-sampling procedure is performed using the inverse convolution operations proposed in [39]. Batch normalization [40] and ReLU [41] activation is followed after the deconvolution. The learning procedure is conducted in a supervised fashion. Noteworthy, since it is almost impossible to learn a continuous spatial distribution magnetic field, we use a quantized version of the original distribution as a label. Technically, we quantize the field distributions into 512×512 gray images, with 256 gray scales for each pixel. The spatial distribution is characterized by the coordinates of pixels within the image. The intensity of pixels reflects the strength of the magnetic field. The field strength is normalized between pixel values of 0 and 255. In this sense, the continuous field

prediction task is translated into image prediction. We use the mean absolute error as our cost function, which is defined, for an $N \times M$ image, as follows

$$\mathcal{C}_1(\hat{\mathbf{p}}, \mathbf{p}) = \frac{1}{N \times M} \sum_{i=1}^{N \times M} |\hat{p}_i - p_i|, \quad (4)$$

where $\hat{\mathbf{p}}$ stands for the pixels predicted via the U-Net model, and \mathbf{p} is the corresponding labels. In practice, we use the smooth mean absolute error introduced in [42], instead of the original form, to smooth the gradients during the optimization procedure.

In terms of optimal parameter prediction, we use an MLP to simultaneously predict the four parameters (Q_1 , M , L_1 , and R_1) in Figure 2, together with the minimal and maximum values (B_{max} and B_{min}) of the magnetic fields, which are used to estimate the actual intensity of the fields. The cost function for our optimal parameter prediction is the mean squared error (MSE)

$$\mathcal{C}_2(\hat{\mathbf{y}}, \mathbf{y}) = \frac{1}{R} \sum_{i=1}^R (\hat{y}_i - y_i)^2, \quad (5)$$

where $\hat{\mathbf{y}}$ represents the predicted parameters, and \mathbf{y} is the ground truth. The overall cost function for the whole task is the weighted sum of these two components

$$\mathcal{C} = \alpha \mathcal{C}_1 + \beta \mathcal{C}_2. \quad (6)$$

3.2. Training Configurations

For training, we use stochastic gradient descent to minimize the cost function. The optimizer is Adam [43], with the learning rate 10^{-4} , $\beta_1 = 0.5$, and $\beta_2 = 0.999$. By using COMSOL, we have generated a dataset comprising 30,000 samples with random parametric configurations of coils. Since the parameters take a wide range of values, it is difficult for the neural network to learn. We normalize the values with the z-score normalization defined in Equation (7), such that they are of mean 0 and standard deviation 1. There, μ denotes the original mean value of the parameters and σ represents the original standard deviation.

$$z = \frac{x - \mu}{\sigma}. \quad (7)$$

The dataset is then partitioned randomly, with 70% of it allocated for model training and the remaining 30% used for validation. The model is trained for 200 epochs in total. When the model is well trained, it can generate gray images of the magnetic field and the optimal parameters given arbitrary unseen inputs within a reasonable time. Note that since the predicted pixel values for magnetic fields are normalized, the minimal and maximum values r_{min} and r_{max} of the strength of the actual field are therefore utilized to generate real intensity. The mapping from pixel values p to actual values r is

$$r = r_{min} + (r_{max} - r_{min}) \times \frac{p}{255}. \quad (8)$$

4. Results of COMSOL and POWPTML

Investigations into wireless power delivery mechanisms for capsules have expanded considerably over recent years as an active domain of inquiry [9,44]. Therefore, based on our past work [45], this paper conducts research on the wireless power supply in wireless capsule endoscopy as a scenario because it usually encounters the problem of insufficient power and energy. WPT offers a viable solution to this problem, and machine learning can be used for more efficient parameter optimization. However, this parameter optimization of WPT based on the machine learning method used for WPT proposed by this paper is not limited to this scenario. The application of the capsule is an example, and it can also be used to find the optimal parameters of WPT in EVs, mobile phones, etc. The proposed method

facilitates the identification of parameter values corresponding to maximum efficiency or calculates the desired parameters, such as inductance and resistance, for a specific coil.

For the wireless power transfer scenario in capsule endoscopy applications, we configured the receiving coil with a diameter of 13.0 mm, a wire diameter of 0.19 mm, and 200 turns. The diameter, wire diameter, and turns of the receiving coil were determined according to recent references [9,46], ensuring the selected parameters are acceptable for the human body. These parameters can determine the value of L_2 and Q_2 . Therefore, they can affect the transmission efficiency of the system, but due to the size of the capsule, only parameters closer to the actual use can be chosen. After performing a COMSOL simulation using the selected parameters, we obtained the results for the receiving coil on the capsule endoscopy, which showed that the inductance L_2 is 229.45 μH , and the quality factor Q_2 is 15.69. The outer diameter, wire diameter, wire spacing, and number of turns of the transmitting coil are all variable in order to solve the optimal transmitting coil parameters. A sectional view of the 3D model in COMSOL can be seen in Figure 3.

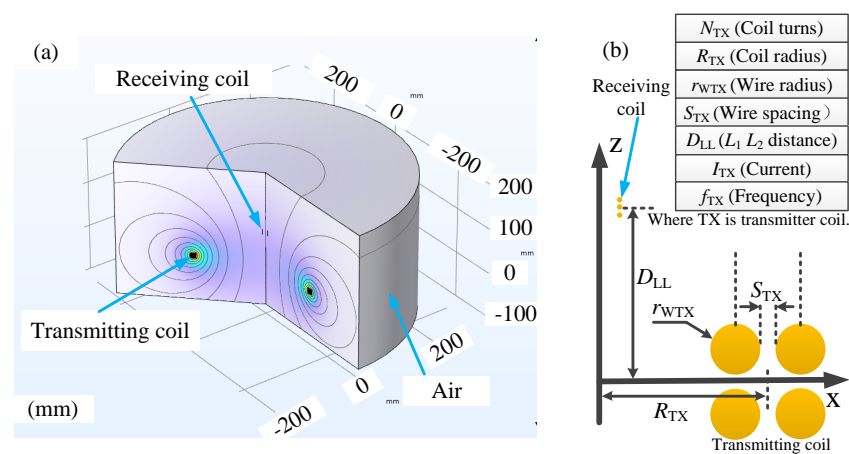


Figure 3. (a) A 3D section model in COMSOL. (b) The definition of parameters in the section of the X–Z plane.

After training a dataset containing a specific amount of data, which was automatically generated via COMSOL with Matlab using random parameters, including N_{TX} , R_{TX} , r_{WTX} , S_{TX} , D_{LL} , I_{TX} , and f_{TX} , we were able to use machine learning to calculate the WPT circuit parameters and magnetic field distribution.

4.1. WPT Efficiency

The trained model can be used for parameter optimization. For example, the wire diameter, the distance between adjacent wires, and the outer diameter of the transmitting coil are 1.9 mm, 0.1 mm, and 300 mm, respectively. When these parameters are determined, we can use our trained model and COMSOL to find the optimal number of turns (N_1) to reach the highest efficiency. The relationship between efficiency and the number of turns (N_1) is calculated via COMSOL and POWPTML, as shown in Figure 4.

The above only compares a comparison of the optimal number of turns calculated via COMSOL and the trained model when the number of turns is variable because the number of turns has a critical effect on WPT. We can also find the optimal parameters of two or more together, such as wire diameter and wire spacing. It is worth noting that the process of finding the optimal parameters for WPT in COMSOL can be time-consuming, as the scan for each circle is time-consuming. In contrast, the trained model provides a more efficient approach to parameter optimization.

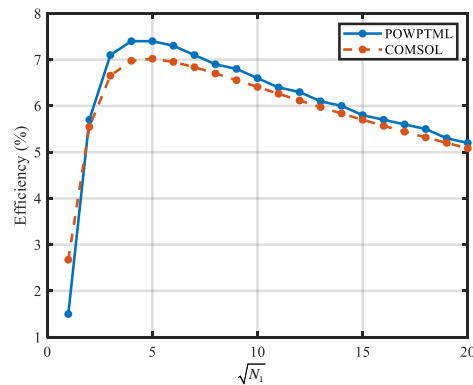


Figure 4. The relationship between efficiency and the number of turns.

To illustrate how to automatically find the optimal parameters, we will present an example using the optimization of the number of turns. The process for finding optimal values for other parameters is similar to this example. First, we use the trained ML model to compute all the circuit parameters of the transmitting coil turns from 1 to N_{max} using Python code, where N_{max} is the specified maximum number of turns. Then, the efficiency values for each number of turns from 1 to N_{max} are computed. The program outputs the number of turns with the maximum efficiency and generates a plot of the relationship between efficiency and the number of turns. A flowchart for this process is shown in Figure 5.

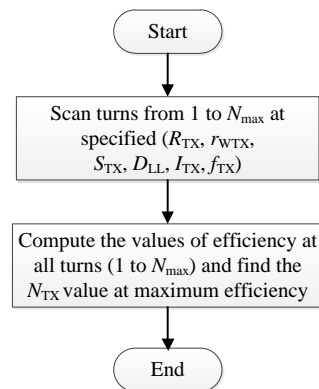


Figure 5. Parameter optimization flow chart of the number of turns.

4.2. Magnetic Field Distribution

Obtaining accurate magnetic field distribution is crucial for ensuring the safety of equipment or the human body in wireless power transfer (WPT) systems. Prior to fabricating the WPT system, we can use COMSOL or POWPTML to calculate the magnetic field distribution. The magnetic field distribution calculated via COMSOL is shown in Figure 6a,c,e, and that calculated via POWPTML is shown in Figure 6b,d,f. The POWPTML method was able to draw the curve of a safe magnetic flux density of $27 \mu\text{T}$, indicating its effectiveness in ensuring the safe operation of the WPT system.

The distribution error in the magnetic field calculation could be attributed to the training process. Since the magnetic field is very weak far from the coil, the pixel values may not be distinguishable, leading to inaccuracies in the calculation. This issue should be further investigated to improve the accuracy of the magnetic field distribution.

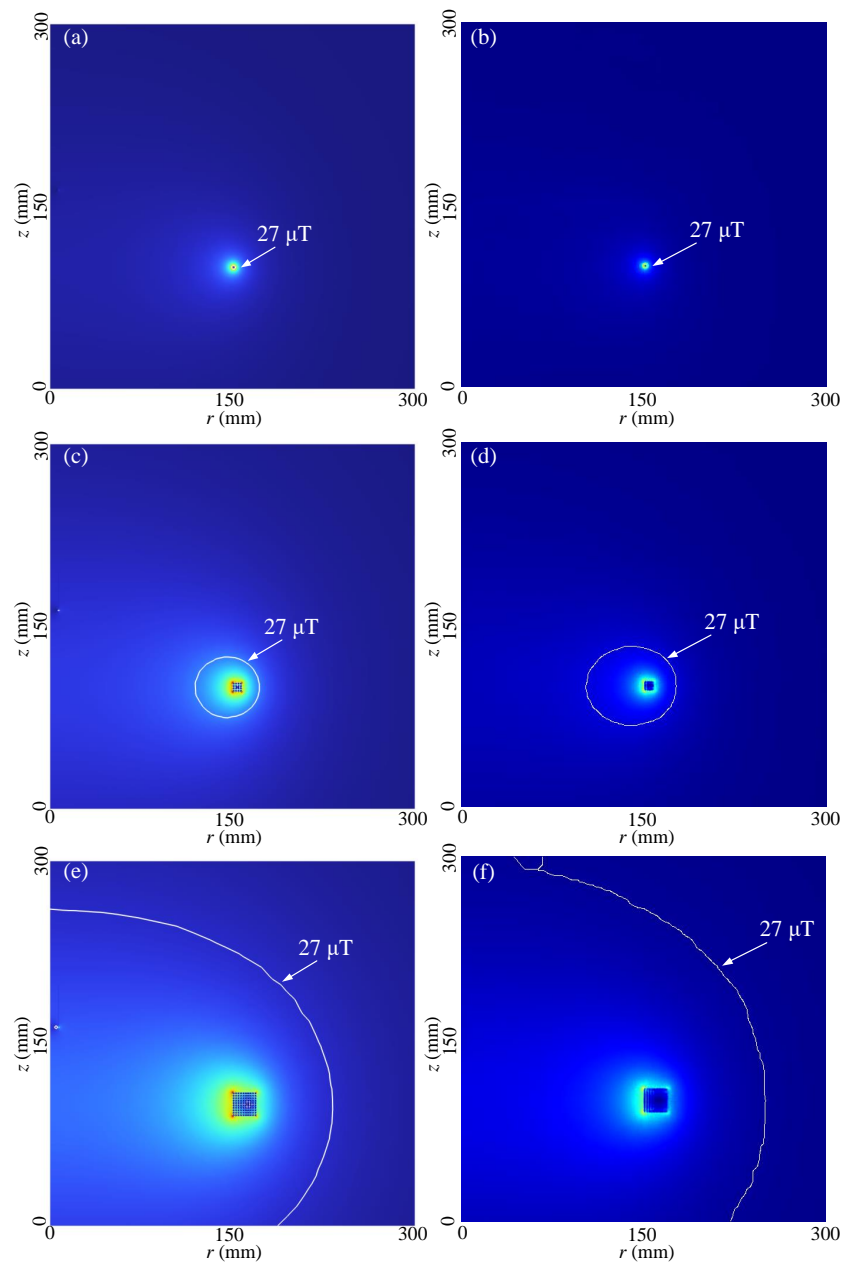


Figure 6. Magnetic field distribution. The current $I_{TX} = 0.2$ A. (a,c,e) The results of COMSOL. (b,d,f) The results of machine learning. In (a,b), $N_{TX} = 1$. In (c,d), $N_{TX} = 16$. In (e,f), $N_{TX} = 100$.

4.3. A Time Comparison of Two Methods

It is crucial to evaluate the time required for each method to complete a given task, as this directly affects the efficiency and practicality of the method. The ability of an algorithm to perform calculations quickly without sacrificing accuracy is a significant advantage in real-world applications. Therefore, computation time plays a critical role in the performance evaluation of different computational methods. In the COMSOL simulation, the CPU used is an Intel(R) Core(TM) I7-12700, and the calculation time is related to the number of turns, as shown in Figure 7a. However, the computation time for the proposed method (POWPTML) is almost unaffected by the number of coil turns, with a calculation time of only about 3 ms each time, as shown in Figure 7b. We used a graphics card, a GeForce RTX 2080 Ti, in our calculations using the POWPTML method.

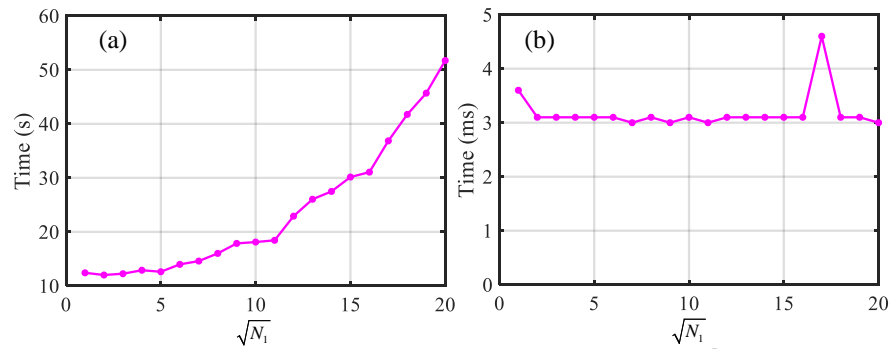


Figure 7. The relationship between calculation time and the number of turns. (a) Computed via COMSOL. (b) Computed via POWPTML.

A time comparison can be seen in Table 2. It is obvious that POWPTML can save a large amount of time when calculating the optimal parameters.

Table 2. Computation of the total time consumed for 20 sets of data between COMSOL and POWPTML.

Method	Time (s)
COMSOL	474.884
POWPTML	0.064

5. Experiments

After acquiring the COMSOL-generated dataset and completing the data model training, the physical system was built and tested in this section.

5.1. Design of Experiments

To experimentally validate our proposed method, a resin bobbin for the capsule receiving coil was fabricated using a 3D printer with an inner diameter of 11 mm, an outer diameter of 13 mm, and a length of 50 mm. The bobbin for the transmitting coils was made using acrylic sheets with an inner diameter of 290 mm, an outer diameter of 300 mm, and a length of 30 mm. In order to verify the effectiveness of the method proposed in this paper, a receiving coil with 200 turns and transmitting coils with different numbers of turns were fabricated to compare the results with the machine learning and finite element methods. In this experiment, we used a network analyzer (E5061B) to measure the inductance (L_1 , L_2), quality factor (Q_1 , Q_2), mutual inductance (M), and resistance (R_1 , R_2). The distance between the transmitting coil and the receiving coil was set to 60 mm. The wire diameter of the transmitting coil was 1.9 mm. When fabricating the coils, we tried to keep the wire diameter, wire spacing, and winding exactly the same for both the simulation and experiment. Figure 8 displays a photograph of the experimental setup.

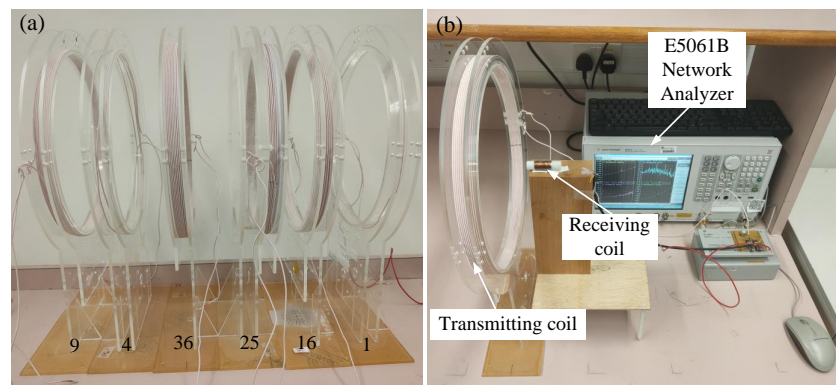


Figure 8. Experimental setup. (a) Transmitting coils with different turns. (b) Test scenario.

5.2. Experimental Results

In the experiment, the parameters of the receiving coil were measured first. The inductance of the receiving coil L_2 was 231.06 μH , the quality factor Q_2 was 36.94, and the resistance was 8.57 Ω . We also measured the parameters of the transmitting coil with turns 1, 4, 9, 16, 25, and 36. Then, the mutual inductance between the transmitting coil and the receiving coil was measured at a center distance of 60 mm. A comparison of these parameters is shown in Figure 9. The errors for POWPTML and experiments using COMSOL, as reference values, are shown in Table 3.

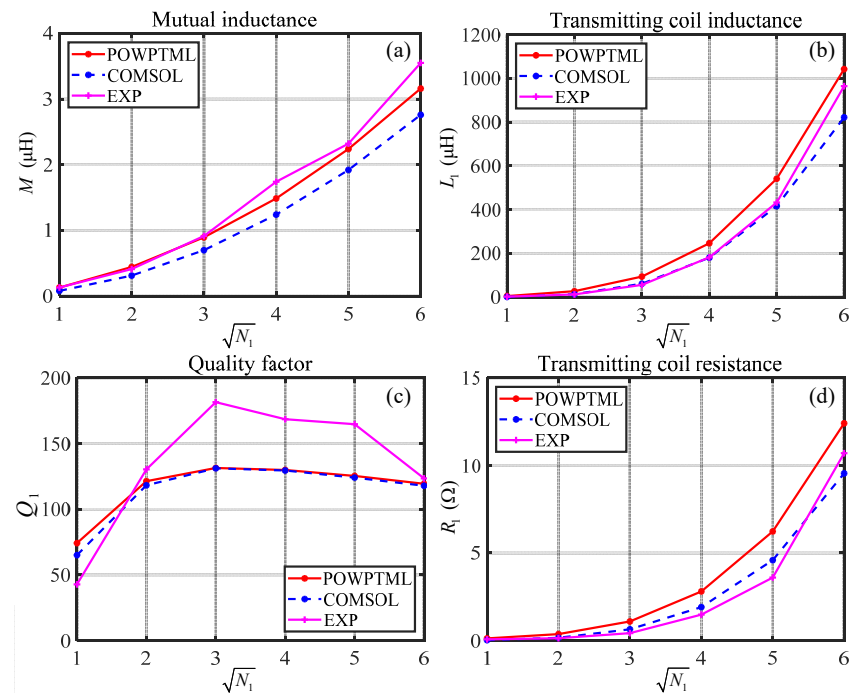


Figure 9. Comparison under different calculation models. (a) Comparison of mutual inductance. (b) Comparison of transmitting coil inductance. (c) Comparison of quality factor. (d) Comparison of transmitting coil resistance.

Table 3. Experimental errors for POWPTML and COMSOL as reference values.

	M (μH)	L_1 (μH)	Q_1	R_1 (Ω)
POWPTML	0.224	77.05	2.62	1.026
Experiment	0.343	28.05	28.36	0.477

Figure 9 shows that there are discrepancies in the coil parameters measured using the three methods, but their respective trends are consistent. This experiment confirms the feasibility of using the ML method to determine the maximum number of turns for efficiency, as well as obtaining quick approximations of the coil parameters. Discrepancies between the experimental and simulated data may be attributed to differences in the winding of the coil, as well as the external wiring used for measurements, which can affect the values of inductance, resistance, quality factor, and mutual inductance. Additionally, training errors may occur during machine learning.

6. Discussion

A magnetic field is an important parameter for energy transfer, and safety constraints need to take the magnetic field into account; thus, the study of magnetic field distribution is of great interest. In this paper, the training data in this paper were generated using a COMSOL simulation, so the results of the proposed method are close to COMSOL data. However, in the future, it is possible to use experimental data for model training to obtain

higher model accuracy relative to experimental data. In addition, measuring the magnetic field before training the model will also be extremely challenging, as mapping the magnetic field distribution may require measuring the magnetic field at hundreds or thousands of points. Therefore, during the experiment and training in this study, we did not experiment with the practical magnetic field part. However, in the future, this part is worthy of being studied. If we can obtain enough experimental data for training the model, our model will be closer to practical application. In practical application, more accurate results will be obtained in the trained model using practical measurement data.

As for the source of error in the magnetic field distribution, it may come from its own computational or modeling errors in COMSOL or from inaccurate parameter tuning during the training process. The tuning of training parameters needs to be adjusted according to the training results to minimize the computational errors in the magnetic field distribution and parameter output. The main limitation of COMSOL is that it is slow at computing and does not automatically find the optimal parameters, while the proposed machine learning method requires a large dataset. A larger dataset is required if a wider range of models is to be applied. The parameters of the experiment and the simulation should be as consistent as possible, but the specific parameters of the experiment cannot be the same as the simulation, as there will always be errors in the wire diameter, coil diameter, and wire spacing.

7. Conclusions

A parameter optimization method for WPT based on machine learning (POWPTML) was presented in this paper. The proposed method was successfully validated through experiments, showing small discrepancies between the hardware measurement and predicted results. After training 30,000 sets of data, the error value of the obtained normalized image prediction using the proposed method was 0.0034. Compared to a commercial tool (i.e., COMSOL), POWPTML's calculation time was much faster and largely independent of the number of turns of the coupled coils, thus significantly speeding up the design and optimization process. The predicted outcome using POWPTML was mostly similar to COMSOL, confirming the accuracy of the proposed method. POWPTML serves as a reliable tool for the rapid design and optimization of WPT systems.

Author Contributions: Conceptualization, H.Z., L.H. and C.-K.L.; methodology, H.Z., M.L., L.H. and C.-K.L.; software, H.Z. and M.L.; validation, H.Z. and M.L.; formal analysis, H.Z. and M.L.; investigation, H.Z. and M.L.; resources, H.Z. and M.L.; data curation, H.Z. and M.L.; writing—original draft preparation, H.Z. and M.L.; writing—review and editing, H.Z. and C.-K.L.; visualization, H.Z., M.L. and C.-K.L.; supervision, C.-K.L.; project administration, C.-K.L.; funding acquisition, C.-K.L. All authors have read and agreed to the published version of the manuscript.

Funding: This research project was supported by the Hong Kong Research Grant Council under the General Research Fund Projects (17210420) and Theme-based Research Scheme (T23-701/20-R).

Data Availability Statement: Data are contained within the article.

Conflicts of Interest: The authors declare no conflicts of interest.

Abbreviations

The following abbreviations are used in this manuscript:

WPT	Wireless power transfer
AI	Artificial intelligence
ML	Machine learning
POWPTML	Parameter optimization of WPT based on machine learning
ICNIRP	The International Commission on Non-Ionizing Radiation Protection
EV	Electric vehicle
SAE	Society of Automotive Engineers
MLP	Multi-layer perceptron

References

1. Cheng, C.; Lu, F.; Zhou, Z.; Li, W.; Zhu, C.; Zhang, H.; Deng, Z.; Chen, X.; Mi, C.C. Load-independent wireless power transfer system for multiple loads over a long distance. *IEEE Trans. Power Electron.* **2018**, *34*, 9279–9288. [\[CrossRef\]](#)
2. Na, W.; Park, J.; Lee, C.; Park, K.; Kim, J.; Cho, S. Energy-efficient mobile charging for wireless power transfer in Internet of Things networks. *IEEE Internet Things J.* **2017**, *5*, 79–92. [\[CrossRef\]](#)
3. Lee, H.; Lee, K.J.; Kim, H.; Lee, I. Wireless information and power exchange for energy-constrained device-to-device communications. *IEEE Internet Things J.* **2018**, *5*, 3175–3185. [\[CrossRef\]](#)
4. Xu, W.; Liang, W.; Peng, J.; Liu, Y.; Wang, Y. Maximizing charging satisfaction of smartphone users via wireless energy transfer. *IEEE Trans. Mob. Comput.* **2016**, *16*, 990–1004. [\[CrossRef\]](#)
5. Li, Y.; Chen, Y.; Chen, C.S.; Wang, Z.; Zhu, Y. Charging while moving: Deploying wireless chargers for powering wearable devices. *IEEE Trans. Veh. Technol.* **2018**, *67*, 11575–11586. [\[CrossRef\]](#)
6. Kim, J.; Kim, D.H.; Choi, J.; Kim, K.H.; Park, Y.J. Free-positioning wireless charging system for small electronic devices using a bowl-shaped transmitting coil. *IEEE Trans. Microw. Theory Tech.* **2015**, *63*, 791–800. [\[CrossRef\]](#)
7. Liu, H.; Huang, X.; Tan, L.; Guo, J.; Wang, W.; Yan, C.; Xu, C. Dynamic wireless charging for inspection robots based on decentralized energy pickup structure. *IEEE Trans. Ind. Inform.* **2017**, *14*, 1786–1797. [\[CrossRef\]](#)
8. Rim, C.T.; Mi, C. *Wireless Power Transfer for Electric Vehicles and Mobile Devices*; John Wiley & Sons: Hoboken, NJ, USA, 2017.
9. Gao, J.; Zhou, J.; Yuan, C.; Zhang, Z.; Gao, C.; Yan, G.; Li, R.; Zhang, L. Stable Wireless Power Transmission for a Capsule Robot with Randomly Changing Attitude. *IEEE Trans. Power Electron.* **2022**, *38*, 2782–2796. [\[CrossRef\]](#)
10. Yan, Z.; Song, B.; Zhang, Y.; Zhang, K.; Mao, Z.; Hu, Y. A rotation-free wireless power transfer system with stable output power and efficiency for autonomous underwater vehicles. *IEEE Trans. Power Electron.* **2018**, *34*, 4005–4008. [\[CrossRef\]](#)
11. Li, H.; Wang, C.; Liu, Y.; Yue, R. Research on single-switch wireless power transfer system based on SiC MOSFET. *IEEE Access* **2019**, *7*, 163796–163805. [\[CrossRef\]](#)
12. Han, G.; Liu, Y.; Guo, S.; Han, T.; Li, Q. Design of coaxial coupled structure for distance-insensitive wireless power transfer. *Rev. Sci. Instruments* **2019**, *90*, 074708. [\[CrossRef\]](#) [\[PubMed\]](#)
13. Guillod, T.; Papamanolis, P.; Kolar, J.W. Artificial neural network (ANN) based fast and accurate inductor modeling and design. *IEEE Open J. Power Electron.* **2020**, *1*, 284–299. [\[CrossRef\]](#)
14. Guillod, T.; Kolar, J.W. Medium-frequency transformer scaling laws: Derivation, verification, and critical analysis. *CPSS Trans. Power Electron. Appl.* **2020**, *5*, 18–33. [\[CrossRef\]](#)
15. Leibl, M. Three-Phase PFC Rectifier and High-Voltage Generator for X-ray Systems. Ph.D Thesis, ETH Zurich, Zurich, Switzerland, 2017.
16. Leibl, M.; Ortiz, G.; Kolar, J.W. Design and experimental analysis of a medium-frequency transformer for solid-state transformer applications. *IEEE J. Emerg. Sel. Top. Power Electron.* **2016**, *5*, 110–123. [\[CrossRef\]](#)
17. Stupar, A.; Taylor, J.A.; Prodic, A. Posynomial models of inductors for optimization of power electronic systems by geometric programming. In Proceedings of the 2016 IEEE 17th Workshop on Control and Modeling for Power Electronics (COMPEL), Trondheim, Norway, 27–30 June 2016; pp. 1–8.
18. Burkart, R.M. Advanced Modeling and Multi-Objective Optimization of Power Electronic Converter Systems. Ph.D Thesis, ETH Zurich, Zurich, Switzerland, 2016.
19. Mogorovic, M.; Dujic, D. 100 kW, 10 kHz medium-frequency transformer design optimization and experimental verification. *IEEE Trans. Power Electron.* **2018**, *34*, 1696–1708. [\[CrossRef\]](#)
20. Guillod, T. Modeling and Design of Medium-Frequency Transformers for Future Medium-Voltage Power Electronics Interfaces. Ph.D Thesis, ETH Zurich, Zurich, Switzerland, 2018.
21. Guillod, T.; Krismer, F.; Kolar, J.W. Magnetic equivalent circuit of MF transformers: Modeling and parameter uncertainties. *Electr. Eng.* **2018**, *100*, 2261–2275. [\[CrossRef\]](#)
22. Le, N.Q.K.; Ou, Y.Y. Incorporating efficient radial basis function networks and significant amino acid pairs for predicting GTP binding sites in transport proteins. *BMC Bioinform.* **2016**, *17*, 183–192. [\[CrossRef\]](#) [\[PubMed\]](#)
23. Ou, Y.Y. Identifying the molecular functions of electron transport proteins using radial basis function networks and biochemical properties. *J. Mol. Graph. Model.* **2017**, *73*, 166–178.
24. Serrano, D.; Li, H.; Guillod, T.; Wang, S.; Luo, M.; Sullivan, C.R.; Chen, M. Neural Network as Datasheet: Modeling BH Loops of Power Magnetics with Sequence-to-Sequence LSTM Encoder-Decoder Architecture. In Proceedings of the 2022 IEEE 23rd Workshop on Control and Modeling for Power Electronics (COMPEL), Tel Aviv, Israel, 20–23 June 2022; pp. 1–8.
25. Tian, F.; Cobaleda, D.B.; Martinez, W. Deep Reinforcement Learning for DC-DC converter parameters optimization. In Proceedings of the 2022 IEEE 31st International Symposium on Industrial Electronics (ISIE), Anchorage, AK, USA, 1–3 June 2022; pp. 325–329.
26. Goodrick, K.J.; Butler, A.; Byrd, T.; Maksimović, D. Machine Learning Estimators for Power Electronics Design and Optimization. In Proceedings of the 2021 IEEE Design Methodologies Conference (DMC), Virtual, 14–15 July 2021; pp. 1–8.
27. Ahlbom, A.; Bergqvist, U.; Bernhardt, J.H.; Cesarini, J.P.; Grandolfo, M.; Hietanen, M.; McKinlay, A.F.; Repacholi, M.H.; Sliney, D.H.; Stolwijk, J.A.; et al. Guidelines for limiting exposure to time-varying electric, magnetic, and electromagnetic fields (up to 300 GHz). *Health Phys.* **1998**, *74*, 494–522.

28. International Commission on Non-Ionizing Radiation Protection. Guidelines for limiting exposure to time-varying electric and magnetic fields (1 Hz to 100 kHz). *Health Phys.* **2010**, *99*, 818–836. [[CrossRef](#)]
29. Mohammad, M.; Onar, O.C.; Pries, J.L.; Galigekere, V.P.; Su, G.J.; Wilkins, J. Analysis of Magnetic Field Emissions and Shield Requirements for Interoperating High-Power EV Wireless Charging System. In Proceedings of the 2021 IEEE Applied Power Electronics Conference and Exposition (APEC), Virtual, 14–17 June 2021; pp. 1586–1592.
30. Wireless Power Transfer for Light-Duty Plug-in/Electric Vehicles and Alignment Methodology. [EB/OL]. Available online: https://www.sae.org/standards/content/j2954_201904/ (accessed on 23 April 2019).
31. Fang, C.; Song, J.; Lin, L.; Wang, Y. Practical considerations of series-series and series-parallel compensation topologies in wireless power transfer system application. In Proceedings of the 2017 IEEE PELS Workshop on Emerging Technologies: Wireless Power Transfer (WoW), Chongqing, China, 20–22 May 2017; pp. 255–259.
32. Aditya, K.; Williamson, S.S. Comparative study of series-series and series-parallel topology for long track EV charging application. In Proceedings of the 2014 IEEE Transportation Electrification Conference and Expo (ITEC), Dearborn, MI, USA, 15–18 June 2014; pp. 1–5.
33. Nanda, N.N.; Yusoff, S.H.; Toha, S.F.; Hasbullah, N.F.; Roszaidie, A.S. A brief review: Basic coil designs for inductive power transfer. *Indones. J. Electr. Eng. Comput. Sci.* **2020**, *20*, 1703–1716.
34. Kurs, A.; Karalis, A.; Moffatt, R.; Joannopoulos, J.D.; Fisher, P.; Soljacic, M. Wireless power transfer via strongly coupled magnetic resonances. *Science* **2007**, *317*, 83–86. [[CrossRef](#)]
35. Goodfellow, I.; Bengio, Y.; Courville, A. *Deep Learning*; MIT Press: Cambridge, MA, USA, 2016.
36. Ronneberger, O.; Fischer, P.; Brox, T. U-Net: Convolutional Networks for Biomedical Image Segmentation. In *Medical Image Computing and Computer-Assisted Intervention—MICCAI 2015: 18th International Conference, Munich, Germany, 5–9 October 2015*; Springer International Publishing: Berlin/Heidelberg, Germany, 2015. [[CrossRef](#)]
37. Haykin, S. *Neural Networks: A Comprehensive Foundation*; Prentice Hall PTR: Hoboken, NJ, USA, 1994.
38. Minaee, S.; Boykov, Y.; Porikli, F.; Plaza, A.; Kehtarnavaz, N.; Terzopoulos, D. Image Segmentation Using Deep Learning: A Survey. *arXiv* **2020**. arXiv:2001.05566. [[CrossRef](#)].
39. Zeiler, M.D.; Krishnan, D.; Taylor, G.W.; Fergus, R. Deconvolutional networks. In Proceedings of the 2010 IEEE Computer Society Conference on Computer Vision and Pattern Recognition, San Francisco, CA, USA, 13–18 June 2010; pp. 2528–2535.
40. Ioffe, S.; Szegedy, C. Batch normalization: Accelerating deep network training by reducing internal covariate shift. In Proceedings of the International Conference on Machine Learning, pmlr, Lille, France, 6–11 July 2015; pp. 448–456.
41. Agarap, A.F. Deep learning using rectified linear units (relu). *arXiv* **2018**, arXiv:1803.08375.
42. Girshick, R. Fast R-CNN. *arXiv* **2015**, arXiv:1504.08083. [[CrossRef](#)].
43. Kingma, D.P.; Ba, J. Adam: A Method for Stochastic Optimization. *arXiv* **2014**, arXiv:1412.6980. [[CrossRef](#)].
44. Meng, Y.; Yan, G.; Jiang, P.; Zhao, K.; Wang, W.; Chen, F.; Zhuang, H. A novel wireless power transfer system with two parallel opposed coils for gastrointestinal capsule robot. *Sens. Actuators A Phys.* **2021**, *321*, 112413. [[CrossRef](#)]
45. Zhang, H.; Li, Y.; Li, Z. 6-D Spatial Localization of Wireless Magnetically Actuated Capsule Endoscopes Based on the Fusion of Hall Sensor Array and IMU. *IEEE Sensors J.* **2022**, *22*, 13424–13433. [[CrossRef](#)]
46. Basar, Md Rubel and Ahmad, Mohd Yazed and Cho, Jongman and Ibrahim, Fatimah. An improved wearable resonant wireless power transfer system for biomedical capsule endoscope. *IEEE Trans. Ind. Electron.* **2018**, *65*, 7772–7781. [[CrossRef](#)]

Disclaimer/Publisher’s Note: The statements, opinions and data contained in all publications are solely those of the individual author(s) and contributor(s) and not of MDPI and/or the editor(s). MDPI and/or the editor(s) disclaim responsibility for any injury to people or property resulting from any ideas, methods, instructions or products referred to in the content.